

X-ray flares and the duration of engine activity in gamma-ray bursts

Davide Lazzati and Rosalba Perna

JILA, University of Colorado, Boulder, CO 80309-0440, USA e-mail: lazzati@colorado.edu, rosalba@jilau1.colorado.edu

22 October 2018

ABSTRACT

The detection of bright X-ray flares superimposed on the regular afterglow decay in *Swift* gamma-ray bursts has triggered theoretical speculations on their origin. We study the temporal properties of flares due to internal dissipation and external shock mechanisms. We first show that at least a sizable fraction of the flares cannot be related to external shock mechanisms, since external shock flares evolve on much longer time scales than observed. We then study flares from internal dissipation, showing that the temporal properties allow us to distinguish the emission of slow early shells from that of late faster shells. We show that, due to the rapid evolution of the detected flares, it is most likely that the flares are produced by relatively fast shells ejected by the central engine shortly before they are observed. This implies that the central engine must be active for, in some cases, as long as one day. We finally discuss the constraints and implications that this observation has on the properties and physics of the inner engine, and we elaborate on possible future observational tests on the flare sample to further understand their origin and physics.

Key words: gamma-ray: bursts — radiation mechanisms: non-thermal

1 INTRODUCTION

The external shock model predicts afterglows characterized by a power-law decay in time, with the possible presence of breaks connecting branches of different slope (Mészáros & Rees 1997). Such changes are due to either geometrical properties of the fireball (geometrical beaming, Rhoads 1999) or to spectral transitions (e.g. from a cooling to a non-cooling electron population, Sari, Piran & Narayan 1998). In the pre-*Swift* era, most afterglows were consistent with the simple version of this model. There were, however, notable exceptions, such as GRB 000301C (Masetti et al. 2000), GRB 021004 (Lazzati et al. 2002), and GRB 030329 (Matheeson et al. 2003). All these bursts displayed optical variability in the form of bumps or wiggles superimposed on the smooth power-law decay.

A number of explanations have been discussed in the literature to account for the variations in the optical afterglow brightness. These include inhomogeneities in the external density (Wang & Loeb 2000; Lazzati et al. 2002; Heyl & Perna 2003), refreshed shocks due to the collision of a late shell of plasma with the external shock material (Rees & Mészáros 1998), angular inhomogeneities in the fireball energy distribution (Nakar, Piran & Granot 2002) and gravitational lensing (Loeb & Perna 1998; Garnavich, Loeb & Stanek 2000). Different mechanisms to produce variability in afterglows can in principle be distinguished through their

temporal and spectral properties. In practice, however, a consensus has not been yet reached due to the lack of unambiguous observations.

More recently, *Swift* observations have revealed that flaring activity is relatively common in the early phases of GRB afterglows, sometimes extending for over a day (e.g., Chincarini 2006; O’Brien et al. 2006). The temporal properties of the flares, their intensity, and their spectra suggest an origin that is unrelated to the external shock (Chincarini 2006; Falcone et al. 2006), at least for a fraction of the bumps. Late episodes of “prompt emission”¹ can have two different origin. One possibility is that the inner engine itself is active for a time as long as the detection time of the X-ray flare. Alternatively, the engine can be short-lived but produce, together with the fast ejecta, a tail of slower material. Such slower material can produce internal dissipation (and therefore prompt emission) at late time. Slow shells ejected immediately after the fast ejecta will not produce an external shock at the canonical external shock radius since the ambient medium has been swept by the external shock produced by the fast ejecta, which develops earlier.

¹ Here and in the following we will call prompt emission all the radiation produced by the outflow inside the external shock. Related mechanisms include, but are not limited to, internal shocks, magnetic dissipation, and comptonization of external photons.

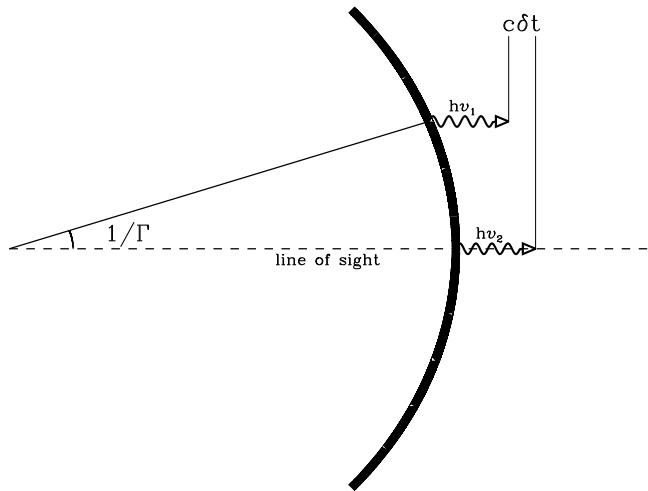


Figure 1. Cartoon showing the geometry of the angular time scale.

Distinguishing between these two scenarios bears important implications for the physics of the GRB engine.

In this paper we discuss the timescales of flares in the different scenarios. We show that at least a large fraction of X-ray flares are due to a long lasting activity of the GRB engine, rather than to external shock activity or to the emission of slow shells immediately after the prompt emission ends.

This paper is organized as follows: in Sect. 2 we compute external shock timescales while in Sect. 3 we consider prompt emission flares and in Sect. 4 we discuss our results and compare them to *Swift* data. We summarize our findings in Sect. 5.

2 EXTERNAL SHOCK

Consider flaring activity produced by a sudden brightening of the external shock. We consider now a brightening that involves the whole surface of the external shock. Even if the duration of the activity in the comoving frame is negligible, the observer at infinity still detects photons over a finite amount of time, due to the “curvature effect” (see Fig. 1). The shape of the observed pulse is therefore the narrowest possible in time. A longer activity in the comoving frame will produce a longer pulse, obtained by convolution of the two functional shapes.

Let us define the quantity $E'(\nu')$ to be the energy released by the unit area of the fireball as a result of the flaring activity, in the comoving frame. The flux received at infinity is given by (see also Kumar & Panaitescu 2000):

$$F_\nu(t) = \frac{1}{4\pi D^2} \frac{E'(\nu/\delta) \delta^2 d\Sigma}{dt_{\text{obs}}}, \quad (1)$$

where D is the distance to the source, $\delta \equiv [\Gamma(1 - \beta \cos \theta)]^{-1}$

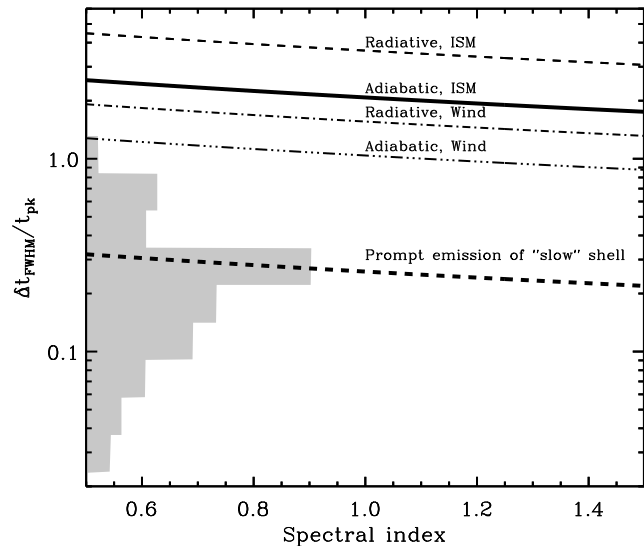


Figure 2. Minimum time scale ratio for flares in different dynamical settings as a function of the spectral index η . From top to bottom, we show a radiative shock propagating into a uniform medium ($\alpha = 3$), an adiabatic shock propagating into a uniform medium ($\alpha = 3/2$), a radiative shock propagating into a wind profile ($\alpha = 1$), an adiabatic shock propagating into a wind profile ($\alpha = 1/2$), and the limit for internal dissipation from a slow shell ejected during or immediately after the prompt phase. The shaded area represents the observational distribution of $\Delta t/t$ from Chincarini (2006), corrected for our Δt definition.

is the Doppler factor, Σ is the fireball surface and t_{obs} the time in the observer frame. This is given by:

$$t_{\text{obs}} = \int_0^R \frac{dr}{\beta_{\text{sh}} c} - \frac{R}{c} \cos \theta \simeq \frac{R}{c} \left[1 - \cos \theta + \frac{1}{2\Gamma_{\text{sh}}^2 (2\alpha + 1)} \right]. \quad (2)$$

Equation (2) holds for any self-similar dynamical evolution where $\Gamma_{\text{sh}} \propto R^{-\alpha}$, as long as $\Gamma_{\text{sh}} \gg 1$. Note that we indicate with the subscript “sh” quantities (such as Lorentz factor and speed) of the external shock, and without subscript the same quantities for the material just behind the shock. It can be shown that $\Gamma_{\text{sh}} = \sqrt{2}\Gamma$ (e.g., Sari 1997).

Easy considerations show that the only non constant quantity in Eq. (1) is the Doppler factor, since $d\Sigma/dt_{\text{obs}} = 2\pi R c$, and all the radiation is emitted at constant radius R . If we assume that we are far from a break in the afterglow spectrum, $E'(\nu') \propto (\nu')^{-\eta}$ and the functional shape of $F_\nu(t)$ can be rewritten as:

$$F_\nu(t) \propto \delta^{(2+\eta)}. \quad (3)$$

Solving Eq. (2) for $\cos \theta$, and expressing time in unit of the start time of the flare $t_0 = R/[2c\Gamma_{\text{sh}}^2(2\alpha + 1)]$, the flare profile can be written as:

$$F_\nu(t) \propto \left(1 + \frac{\tau - 1}{4\alpha + 2} \right)^{-(\eta+2)}, \quad (4)$$

where $\tau = t/t_0$.

Equation 4 can be used to provide a lower limit to an observationally sound definition of the flare duration. Defining the duration as the Full Width at Half Maximum (FWHM) of the pulse, and the reference time as the time t_{pk} of the flare maximum, we obtain:

$$\frac{\Delta t}{t} \equiv \frac{\Delta t_{\text{FWHM}}}{t_{\text{pk}}} \geq \left(2^{\frac{1}{\eta+2}} - 1\right) (4\alpha + 2). \quad (5)$$

Equation (5) depends on both the dynamics and spectrum of the external shock. A steeper spectrum and/or a more slowly evolving fireball will cause a narrower flare. Note that in this case (i.e. impulsive rebrightening of the shock), the maximum coincides with the start time. Should the activity in the comoving frame last for a finite amount of time, a rising phase would be observed. A more detailed treatment, including the width of the shell of shocked material would also provide a profile with a finite rising time. Figure 2 shows the time scale ratio for four typical values of α as a function of the spectral index. The most relevant case for X-ray flares is the adiabatic ISM case, with a spectral slope $\eta \sim 1.2$. We find for that specific case: $\Delta t/t \gtrsim 2$.

In an analogous context, Zhang et al. (2006) discussed the possible production of flares by various mechanisms such as density bumps, post-energy injection in the blast wave, and two-components or patchy jets. In all cases, they concluded that the characteristics of the flares were not generally consistent with what predicted by these models (i.e. $\Delta t/t \sim 1$ and a slower-than observed flux decline). Here, we have derived detailed, quantitative, upper limits on the value of $\Delta t/t$. Our constraints are somewhat tighter than what previously derived by different authors in the context of the external model for flares (e.g., Ioka, Kobayashi & Zhang 2005) but comparable to more recent results (Wu et al. 2006). Our method differs in two important ways from what done in previous work. First, we have computed the actual functional shape of the flare, and defined rigorously the time reference we adopt (the peak) and the time width (the FWHM). In previous works, these quantities were usually poorly defined, and the results could only be approximate. Secondly, we considered the difference between the Lorentz factor of the shock and that of the shocked material. This factor by itself leads to flares which are broader by a factor of two.

Chincarini (2006) presents a distribution of $\Delta t/t$ for a sample of *Swift* X-ray flares that is defined as the ratio of the Gaussian σ over the peak time. The distribution is shown in their Fig. 8 and shaded in Fig. 2. Since for a Gaussian the *FWHM* is equal to 2.35σ , we can easily convert their definition of Δt into our definition. We conclude that the distribution of $\Delta t/t$ of *Swift* X-ray flares is characterized by $0.02 \lesssim \Delta t/t \lesssim 1.3$ and has average $\Delta t/t = 0.3$. Considering Fig. 2, we conclude that most, if not all, the detected rebrightenings are not related to events taking place on the external shock, unless only a small portion of the shock is involved in the rebrightening. Flares caused by a small portion of the shock are possible, but are unlikely to be very strong. Nakar & Granot (2006) studied the effect of a blob of high density interacting with the shock. They find that the rebrightening is minor, and characterized by a very slow rise. Alternatively, a large rebrightening on a small timescale can be observed if a narrow opening angle shell refreshes a small part of the external shock (Granot, Nakar & Piran 2003). This is not likely to be the case for the *Swift* X-ray flares, since most of them are observed before the jet break time (Chincarini 2006, O'Brien 2006) and the opening angle of the jet grows with time (Lazzati & Begelman 2005; Morsony, Lazzati & Begelman 2006) rather than decrease.

3 PROMPT EMISSION

Since the largest majority of flares is unlikely to be produced within the external shock, it must be produced during the initial phase of internal dissipation. In the following we therefore discuss flaring activity in the context of the prompt emission. In this case one can envisage two possible scenarios for their production: (a) shells that are produced during the GRB phase but that dissipate at much later times; (b) shells produced at late times by a long-lived engine and dissipating on a timescale comparable to that of the engine duration. Zhang et al. (2006) also concluded that the flares have an internal origin, but directly assumed that the engine must have been long-lived. In this section we try to discriminate between the scenarios (a) and (b). Being able to discriminate between these two scenarios bears important implications for our understanding of the physics of the inner GRB engine (see more discussion on this in §4). In the following, we discuss the two scenarios above, provide diagnostics for each of them, and show that the current *Swift* data is already able to discriminate between the two flare-production mechanisms.

(a) *Flaring activity due to dissipation within a freely expanding flow, released during the prompt GRB phase or shortly afterwards.* This case has two important differences with respect to the external shock case studied above. First, there is no propagating shock, and therefore there is no distinction between Γ and Γ_{sh} . Second, the flare is produced by material that has been coasting at constant Γ , rather than by material that has been slowing down. These two differences change considerably the equations above.

Without repeating the derivation of Sect. 2, it can be easily seen that the result for the freely expanding flow can be obtained by substituting $4\alpha + 2$ with $2\alpha + 1$ and adopting $\alpha = 0$ in Eq. 5. This yields:

$$\frac{\Delta t_{\text{FWHM}}}{t_{\text{pk}}} \gtrsim 2^{\frac{1}{2+\eta}} - 1, \quad (6)$$

which, for the typical case of $\eta \sim 1.2$ yields $\Delta t/t \gtrsim 0.25$ (see Wu et al. 2006 for a similar computation restricted to the case of internal shocks). This number is tantalizing similar to the average width of *Swift* X-ray flares (Chincarini 2006; Fig. 2). Yet, there is a sizable number of events for which the condition is violated by almost an order of magnitude. In addition, should the condition be barely satisfied, the decay part of the flare would be dominated by large angle emission (Kumar & Panaitescu 2000; Liang et al. 2006). This seems not to be the case, at least in some of the flares (Guetta et al. 2006). Note however that the large angle emission should not dominate any flare with a duration significantly larger than the one given in Eq. (6).

(b) *Shell that is ejected from the central engine after a time t_{ej} sizably larger than the prompt emission timescale T_{90} .* If radiation is released at radius R , it will be observed at a time (cfr. Eq. 2)

$$t_{\text{obs}} = t_{\text{ej}} + \frac{R}{c} \left(1 - \cos \theta + \frac{1}{2\Gamma^2}\right), \quad (7)$$

which produces a shortening of the observed variability timescale

$$\frac{\Delta t}{t} \gtrsim \left(2^{\frac{1}{2+\eta}} - 1\right) \left(1 - \frac{t_{\text{ej}}}{t_{\text{pk}}}\right). \quad (8)$$

Equation (8) allows for any arbitrarily small time scale, as long as the shell that produces radiation is ejected at a time comparable to the detection time. Therefore, the detection of fast flares implies that the inner engine is active for a time much longer than the canonical prompt phase (T_{90}).

The observation of a flare that peaks at time t_{pk} and is characterized by a width Δt allows us to constrain the time at which it was ejected from the central engine:

$$1 - \frac{1}{2^{\frac{1}{2+\eta}} - 1} \frac{\Delta t}{t} \lesssim \frac{t_{\text{ej}}}{t_{\text{pk}}} \leq 1. \quad (9)$$

4 DISCUSSION

Equations (6) and (8) are general and hold for any dissipation and radiation mechanism that take place in the whole jet. Locally beamed emission mechanisms can produce fast variability (see, e.g., Lyutikov & Blandford 2004), but the peak luminosity of the flares would drop faster than observed as a function of t_{pk} . Consider now the flares observed by *Swift* (for a recent review, see <http://www.swift.ac.uk/rs06/Burrows.pdf>). They can be observed up to $\sim 10^5$ s after the GRB onset and are characterized by a FWHM time $\delta t \sim 0.3t$. Applying this observational constraint implies that at least in about half of the cases the ejection time of the material from the central engine is comparable to the time at which the flare is observed. In other words, GRB engines are active well beyond the observed T_{90} of the prompt emission, in some cases for up to $\sim 10^5$ s or a day timescale.

This provides an important constraint to the properties of the inner engine of long duration GRBs. More can be obtained by further analysis of the properties of the flares. Flares are observed over a wide range of times, spanning about three orders of magnitude (from 100 to 10^5 s after the end of the prompt emission). The distribution of $\delta t/t$ is however much narrower, spanning approximately only one order of magnitude. This implies a correlation between the ejection time and the duration of the ejection episode. The longer is the time after the engine turns on, the longer is the ejection episode. Interestingly, an analogous property was noted in GRBs with multiple prompt emission episodes (Ramirez-Ruiz & Merloni 2001). During the prompt phase, the duration of an emission episode is strongly correlated with the length of the quiescent time that precedes it. In the case of flares we can conclude that the correlation is with the total time since the engine onset; however, this does not imply the absence of a correlation with the length of the quiescent time.

Our results bear important implications for an understanding of the physical processes governing the GRB inner engine, which provides the ultimate source of energy to power GRBs. The GRB “inner engine” is believed to be a hyperaccreting accretion disk. In the collapsar model (Paczynsky 1998; MacFadyen & Woosley 1999), this is formed by the fallback material from the collapsing envelope of the massive star, and the timescale for the duration of the accretion episode is set by the dynamical timescale of the collapsing envelope itself, which is on the order of several tens of seconds. On the other hand, in the binary merger model (e.g. neutron star-neutron star or neutron star-black hole; Eichler et al. 1989), the accretion material is provided by the debris

of the tidally disrupted neutron star (or white dwarf). In this case, the timescale over which the available material is accreted is set by the viscous timescale of the disk, which is a fraction of a second.

The accretion timescale in the collapsar model easily accounts for the duration of the prompt emission for the class of long bursts, while the accretion timescale in the binary merger model naturally yields the required timescales for the prompt emission of short bursts. Several types of observations in the last few years have indeed provided a strong support for the association between long GRBs and the collapse of a massive star (Stanek et al. 2003; Hjorth et al. 2003), while several pieces of evidence are gradually mounting toward the association of compact-object mergers and short bursts (Fox et al. 2005; Bloom et al. 2006; Nakar, Gal-Yam & Fox 2006).

In the scenarios above, a relativistic outflow is ejected from the central engine, and radiation is produced as the bulk kinetic energy is dissipated and radiated at a given radius. There is no a-priori constraint on the distribution of the Lorentz factor in the outflow. If the Lorentz factor of the ejecta should decrease with the ejection time, late time internal activity could be seen without the need for a long-living engine. We have shown that this is not the case, at least in a sizable fraction of the flares. This result makes the studies of possible mechanisms of reactivation of the GRB engine especially timely. King et al. (2005) suggested that fragmentation of the collapsing star could explain a (single) flare in the case of long bursts, while Dai et al. (2006) proposed a new mechanism of binary merger that can incorporate the presence of a flare for short bursts. Perna, Armitage & Zhang (2006) noted that the fact that flares are observed in both long and short bursts, and with similar characteristics in both cases, is suggestive that the place of formation be in what is common between the two classes of bursts, i.e. the accretion disk. A disk that fragments as a result of gravitational instabilities in its outer parts, as supported by studies of hyperaccreting disks (Di Matteo, Perna & Narayan 2002; Chen & Beloborodov 2006), can account for flares with similar properties in both long and short bursts, as well as accounting for the observed correlation between the flare duration and its arrival time (see also Piro & Pfahl 2006). Other disk-based models involve magnetic instabilities (Proga & Zhang 2006; Giannios 2006). Staff, Ouyed & Bagchi (2006) proposed instead a mechanism based on state transitions in the quark-nova scenario, while the role of a magnetar was discussed by Gao & Fan (2006) and Cea (2006).

4.1 Refreshed shocks

If an “internal” flare, i.e., a flare due to internal dissipation, is observed in a GRB, it must be followed at later time by an external flare. The material responsible for the internal flare keeps expanding at constant speed, and must eventually catch up with the external shock, which decelerates continuously. It may however be difficult to observe the second flare, since it may be weak and dispersed over several orders of magnitudes in time. If, however, the second flare can be singled out and firmly associated to an external flare, it would provide additional important information for our understanding of the dynamics of the system.

Consider a flare system made by an internal flare beginning at time t_{int} followed by a second, broader, flare starting at time t_{ext} , where $t_{\text{ext}} \gg t_{\text{int}}$. The external flare time can tell us the Lorentz factor of the material producing the internal flare:

$$\Gamma_{\text{ej}} \simeq \left(\frac{3E}{8\pi n m_p c^5} \right)^{1/8} t_{\text{ext}}^{-3/8}, \quad (10)$$

where E is the isotropic equivalent kinetic energy of the fireball integrated up to the time of ejection of the late shell, n the numeric density of the external medium, and m_p the proton mass. We have assumed a uniform external medium. Equations can be easily generalized to an arbitrary density profile, but will be simple only in the case of adiabatic evolution. Equation (10) depends only on measurable quantities. An example of a solvable system is the flare system of GRB 050502B. Falcone et al. (2006) were able to identify an initial strong flare and a possible refreshed shock flare at later times. They were able to measure the bulk Lorentz factor of the late engine ejecta to be $\Gamma_{\text{ej}} \lesssim 20$, ejected from the inner engine approximately 300 second after the onset. By itself this observation only tells us that the late ejections are likely to have a smaller Lorentz factor than the early ones. Solving a large numbers of flare systems in different GRBs would however provide us with an ensemble of late ejections that would allow us to constrain both the properties of the engine and of the dissipation/radiation mechanism. The knowledge of the bulk Lorentz factor of the late shells would provide us with a sample of flares for which the comoving spectra are known, ridding the prompt emission models of one of the unknown parameters: the Lorentz factor.

5 SUMMARY

We have analyzed the timescale of flares produced by several mechanisms both due to internal dissipation and external shock phenomena. We have shown that all prominent external shock flares occurring before the jet break must have a long time scale $\delta t \gtrsim t$. We also showed that internal dissipation taking place in slow shells ejected immediately after the end of the prompt phase must satisfy a similar constraint: $\delta t \gtrsim 0.25t$. The only mechanism capable of producing flares with a short time scale as observed by *Swift* is identified with late activity of the inner engine. As a consequence, the detection of X-ray flares at times as long as 10^5 seconds after the GRB onset implies that the inner engine is active for at least 10^5 s. This has important implications for the fueling of the engine and the ejection mechanism.

ACKNOWLEDGEMENTS

We thank Dafne Guetta and Luigi Piro for useful conversations. This work was supported by NASA Astrophysical Theory Grant NNG06GI06G (DL), NSF grant AST-0307502 (DL) and AST 0507571 (DL & RP), and *Swift* Guest Investigator Program NNX06AB69G (DL) and NNG05GH55G (DL & RP).

REFERENCES

- Bloom J. et al. 2006, ApJ, 638, 354
 Cea P., 2006, ApJ in press (astro-ph/0606086)
 Chen W.-X., Beloborodov A. M., 2006, ApJ in press, (astro-ph/0607145)
 Chincarini G., 2006, Proceedings of the Vulcano Workshop 2006, Vulcano, Italy, May 22-27, Edited by F. Giovannelli & G. Mannocchi (astro-ph/0608414)
 Dai Z. G., Wang X. Y., Wu X. F., Zhang B., 2006, Science, 311, 1127
 Di Matteo T., Perna R., Narayan R., 2002, ApJ, 579, 706
 Eichler D., Livio M., Piran T. Schramm D. N., 1989, Nature, 340, 126
 Falcone A. D., et al., 2006, ApJ, 641, 1010
 Fox D. B., et al., 2005, Nature, 437, 845
 Gao W.-H., Fan Y.-Z., 2006, ChJAA, 6, 513
 Garnavich P. M., Loeb A., Stanek K. Z., 2000, ApJ, 544, L11
 Giannios D., 2006, A&A, 455L, 5
 Granot J., Piran T., Sari R., 1999, ApJ, 513, 679
 Granot J., Nakar E., Piran T., 2003, Nature, 426, 138
 Guetta D., D'Elia V., Fiore F., Conciatore M. L., Antonelli L. A., Stella L., 2006, Il Nuovo Cimento in press (astro-ph/0610512)
 Heyl J. S., Perna R., 2003, ApJ, 586L, 13
 Hjorth J., et al., 2003, Nature, 423, 84
 Ioka K., Kobayashi S., Zhang B., 2005, ApJ, 631, 429
 King A., O'Brien P. T., Goad M. R., Osborne J., Olsson E., Page K., 2005, ApJ, 630L, 113
 Kumar P., Panaitescu A., 2000, ApJ, 541, L51
 Lazzati D., Rossi E., Covino S., Ghisellini G., Malesani D., 2002, A&A, 396L, 5
 Lazzati D., Begelman M. C., 2005, ApJ, 629, 903
 Liang E. W., et al., 2006, ApJ, 646, 351
 Loeb A., Perna R., 1998, ApJ, 495, 597
 Lyutikov M., Blandford R., 2004, ASPC, 312, 449
 Matheson T., et al., 2003, ApJ, 599, 394
 MacFadyen A. I., Woosley S. E., 1999, ApJ, 524, 262
 Masetti N., et al., 2000, A&A, 359, L23
 Mészáros P., Rees M. J., 1997, ApJ, 476, 232
 Morsony B. J., Lazzati D., Begelman M. C., 2006, ApJ submitted (astro-ph/0609254)
 Nakar E., Piran T., Granot J., 2003, NewA, 8, 495
 Nakar E., Granot J., 2006, MNRAS submitted (astro-ph/0606011)
 Nakar E., Gal-Yam A., Fox D. B., 2006, ApJ, 650, 281
 O'Brien P. T., et al., 2006, ApJ, 647, 1213
 Paczyński B., 1998, ApJ, 494L, 45
 Perna R., Armitage P. J., Zhang B., 2006, ApJ, 636L, 29
 Piro A. L., Pfahl E., 2006, ApJ submitted (astro-ph/0610696)
 Proga D., Zhang B., 2006, MNRAS, 370L, 61
 Ramirez-Ruiz E., Merloni A., 2001, MNRAS, 320, L25
 Rees M. J., Meszaros P., 1998, ApJ, 496, L1
 Rhoads J. E., 1999, ApJ, 525, 737
 Sari R., 1997, ApJ, 489, L37
 Sari R., Piran T., Narayan R., 1998, ApJ, 497, L17
 Staff J., Ouyed R., Bagchi M., 2006, ApJ submitted (astro-ph/0608470)
 Stanek K., et al. 2003, ApJ, 591L, 17
 Wang X., Loeb A., 2000, ApJ, 535, 788
 Wu X. F., Dai Z. G., Wang X. Y., Huang Y. F., Feng L. L., Lu T., 2006, ApJ submitted (astro-ph/0512555)
 Zhang B., et al., 2006, ApJ, 642, 370